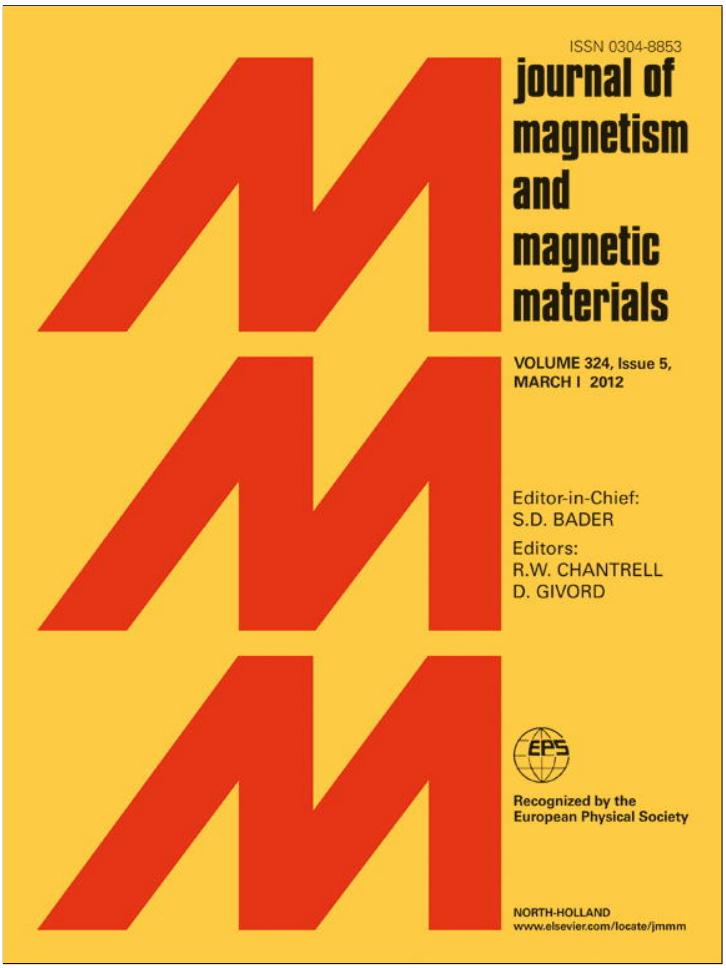

Journal of Magnetism and Magnetic Materials 324 (2012) 723–728

Contents lists available at SciVerse ScienceDirect

Journal of Magnetism and Magnetic Materials

journal homepage: www.elsevier.com/locate/jmmm

Magnetoelastic properties of $ErMn_6Sn_6$ intermetallic compound

Sh. Tabatabai Yazdi [a], N. Tajabor [a,*], M. Rezaee Roknabadi [a], M. Behdani [a], F. Pourarian [b]

[a] Department of Physics, Faculty of Sciences, Ferdowsi University of Mashhad, Mashhad 91775-1436, Iran
[b] Department of Materials Science & Engineering, Carnegie Mellon University, Pittsburgh, PA 15213, USA

ARTICLE INFO

Article history:
Received 16 June 2011
Received in revised form
14 August 2011
Available online 16 September 2011

Keywords:
Rare-earth intermetallic compound
Magnetic phase transition
Magnetostriction
Thermal expansion

ABSTRACT

The thermal expansion and magnetostriction of polycrystalline sample of the $ErMn_6Sn_6$ intermetallic compound with hexagonal $HfFe_6Ge_6$-type structure are investigated in the temperature range of 77 K to above 400 K. The thermal expansion measurement of the sample shows anomalous behavior around its $T_N = 340$ K. The isofield curves of volume magnetostriction also reveal anomalies at paramagnetic–antiferromagnetic and antiferromagnetic–ferrimagnetic phase transitions. In the antiferromagnetic state, the transition to ferrimagnetism can be induced by an applied magnetic field. The threshold field for the metamagnetic transition H_{th} increases from 0.18 T at 84 K to about 1 T around 220 K, and then decreases monotonously to T_N. This behavior is well consistent with that observed earlier on magnetization curves attributed to exchange-related metamagnetic transition rather than the anisotropy-related one. Furthermore, the low H_{th} values suggest that the Mn–Mn coupling in $ErMn_6Sn_6$ is not so strong. The experimental results obtained are discussed in the framework of two-magnetic sublattice by bearing in mind the lattice parameter dependence of the interlayer Mn–Mn exchange interaction in this layered compound. From the temperature dependence of magnetostriction values and considering the magnetostriction relation of a hexagonal structure, we attempt to determine the signs of some of the magnetostriction constants for this compound.

1. Introduction

The RMn_6Sn_6 intermetallic compounds (with R=Sc, Y, Gd–Tm and Lu) have been widely studied during the recent years, using a wide variety of methods, including magnetization measurements [1–3], neutron diffraction [4], Mössbauer spectroscopy [4], NMR spectroscopy [5], transport, magnetotransport [6] and magneto-optical measurements [7], and also some theoretical studies on electronic structure calculations [8]. All these compounds crystallize in the hexagonal $HfFe_6Ge_6$-type structure with space group P6/mmm (Fig. 1): Hf at 1(a) (0, 0, 0), Fe at 6(i) (1/2, 0, $z \approx 1/4$), Ge at 2(c) (1/3, 2/3, 0), 2(d) (1/3, 2/3, 1/2) and 2(e) (0, 0, $z \approx 1/3$). This crystal structure can be described as layers of R and Mn atoms alternately stacked along the *c*-axis in the sequence Mn–(R,Sn)–Mn–Sn–Sn–Sn–Mn [9]. The magnetic structure of RMn_6Sn_6 compounds consists of two different subsystems: the R and Mn subsystems. The observed complex magnetic behavior of these compounds, characterized by various magnetic phase transitions below the magnetic ordering temperature, originates from the complicated interplay among the Mn–Mn, R–Mn and R–R exchange interactions as well as the competing magnetocrystalline anisotropies of the two sublattices. The (001) Mn planes have ferromagnetic ordering, the interlayer Mn–Mn coupling through the Mn–Sn–Sn–Sn–Mn is always positive (ferromagnetic) while the nature of that within the Mn–(R, Sn)–Mn slab depends on the R element. It is believed that these interlayer Mn–Mn interactions depend strongly on the Mn–Mn interatomic distances (for larger distances they are usually positive, while for smaller ones they are negative) and so are very sensitive to the R element [10]. The RMn_6Sn_6 compounds with R=Gd−Ho are ferrimagnetic below their Curie temperature, while ones with R=Sc, Y, Tm and Lu display antiferromagnetic or helimagnetic behaviors. Among them, the compound with R=Er has a complex behavior displaying several transitions. $ErMn_6Sn_6$, in addition to spontaneous (temperature-induced) transitions characterized by antiferromagnetism below $T_N = 352$ K and a transition to ferrimagnetic state at about 75 K, has metamagnetic (field-induced) transitions in its ordered state [1]. Since the Mn sublattice favors an easy plane anisotropy and Er reveals an easy plane behavior in the whole ordered state [4] too, there is no competition between the two sublattices anisotropies and consequently no spin reorientation process in $ErMn_6Sn_6$. The antiferromagnetic–ferrimagnetic transitions in this compound involve transitions from the antiparallel arrangement of Mn-layer moments to the parallel one. Because of the strong interatomic distance dependence of Mn–Mn interlayer interactions, one may expect that these transitions are likely to be

* Corresponding author. Tel.: +98 511 8817741; fax: +98 511 8763647.
E-mail addresses: tajabor@ferdowsi.um.ac.ir, ntajabor@yahoo.com (N. Tajabor).

0304-8853/$ - see front matter © 2011 Elsevier B.V. All rights reserved.
doi:10.1016/j.jmmm.2011.09.004

accompanied by some anomalies in the thermal expansion as well as magnetostriction measurements. To date, no report has been published on magnetoelastic properties of RT_6X_6 compounds (T=Mn, Fe and X= Ge, Sn). Therefore, in the present work, we have investigated the thermal expansion and magnetostriction effects of $ErMn_6Sn_6$ compound.

2. Experiments

The $ErMn_6Sn_6$ polycrystalline sample was prepared by arc melting the constituent elements under high-purity Ar atmosphere in a water-cooled copper boat. The raw materials used were at least of 99.9% purity. The ingot was turned over and remelted several times to insure its homogeneity. The synthesized ingot wrapped in a tantalum foil was sealed in an evacuated quartz tube, annealed at 1023 K for 4 weeks and then quenched in water to obtain a single-phase material. The purity and microstructure of the prepared sample was checked using X-ray powder diffraction (XRD) with monochromatic Cu Kα radiation ($\lambda\sim1.5406$ Å) in the 2θ range of 20–90° in a continuous scan mode with a step width of 0.05° and using scanning electron microscopy (SEM; Leo 1450VP, Carl Zeiss SMT, Germany). For structural characterization, analysis of the obtained XRD profile was performed using the Rietveld refinement method, through the Fullprof software. In order to reveal the magnetic phase transitions, the thermomagnetic measurement was carried out using a LakeShore 7000 magneto-susceptometer with an ac magnetic field of 50 A/m peak value at 125 Hz in the temperature range of 77–330 K. The linear thermal expansion TE normalized to 77 K ($dl/l=(l_T-l_{77\ K})/l_{77\ K}$) and magnetostriction (MS) were measured using the strain-gage Wheatstone bridge technique on disk-shaped samples with a diameter of about 6 mm and thickness of about 2 mm in the temperature range of 77–440 K and magnetic fields up to 1.5 T. The accuracy of these measurements was better than 2×10^{-6}. The longitudinal ($\lambda_{\parallel}$) and transverse magnetostriction ($\lambda_{\perp}$) of the sample were measured parallel and perpendicular to the applied magnetic field, respectively. The anisotropic magnetostriction (λ_t) and the volume magnetostriction (ω) were calculated directly from the relations $\lambda_t=\lambda_{\parallel}-\lambda_{\perp}$ and $\omega=\lambda_{\parallel}+2\lambda_{\perp}$, respectively.

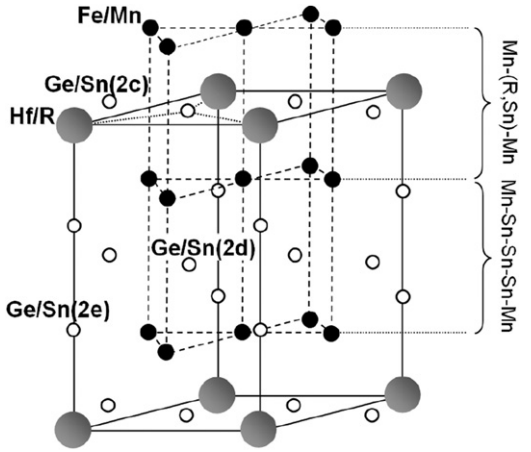

Fig. 1. Representation of the $HfFe_6Ge_6$-type crystal structure of RMn_6Sn_6 compounds.

3. Results and discussion

The XRD pattern indicates that the sample has almost pure single-phase $HfFe_6Ge_6$-type structure (S.G. P6/mmm) with a small amount of β-Sn, Er_2O_3 and Mn_3Sn_2. The presence of such minor impurity phases has been reported in most previous attempts to prepare RMn_6Sn_6 samples by arc-melting or the solid-state reaction method, for instance Refs. [11,12]. The refined lattice parameters using the Rietveld analysis (see for instance [13]) are $a=5.527(4)$ Å, $c=9.020(4)$ Å and the corresponding unit-cell volume $V=238.6(7)$ Å^3, and the c/a ratio equals 1.632, which are well close to the reported values in the literature [14]. The XRD profile lines were modeled using the pseudo-Voigt peak-shape function (the refined Caglioti parameters are $U=0.0078$, $V=-.0079$ and $W=0.0519$). The low values of reliability factors indicate a good refinement (the R-factors are $R_p=7.56\%$, $R_{wp}=10.2\%$, $R_{exp}=5.71\%$ and $\chi^2=(R_{wp}/R_{exp})^2=3.16$). Fig. 2 displays the resultant profile fit of the observed pattern together with the calculated one and the differences between them. The SEM microstructural analysis shows that the prepared sample contains mainly grains of $ErMn_6Sn_6$ phase with the mean size of

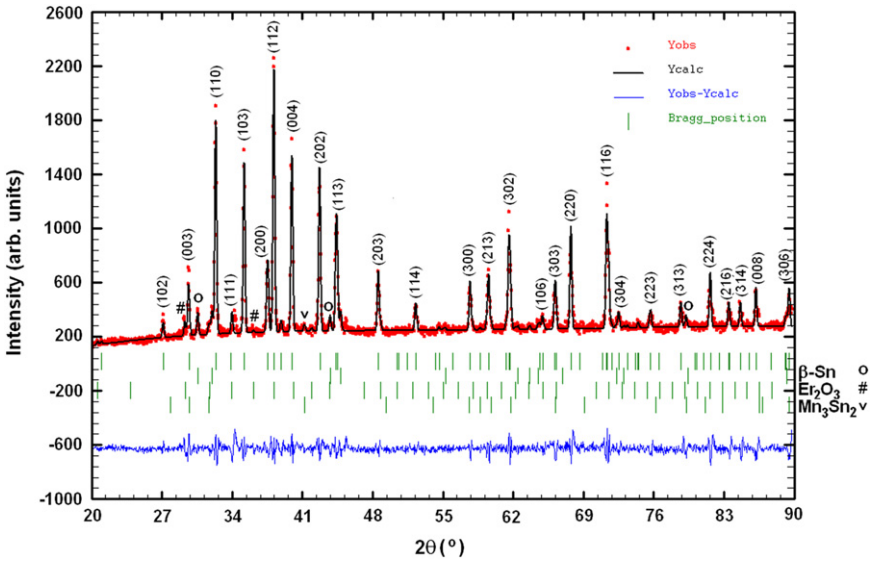

Fig. 2. Observed (circles) and calculated (solid lines) XRD pattern of the $ErMn_6Sn_6$ sample at room temperature. The vertical bars indicate the position of Bragg reflections (upper ticks mark $ErMn_6Sn_6$ lines and the lower ones belong to impurity phases). The difference between the observed and calculated intensities is given at the bottom of the diagram.

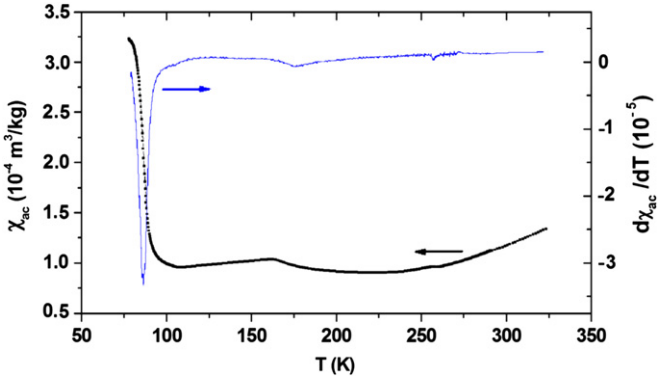

Fig. 3. Temperature dependence of the ac susceptibility χ_{ac} of the $ErMn_6Sn_6$ sample with an ac magnetic field of 50 A/m peak value at 125 Hz and under a zero dc magnetic field, and its first derivative.

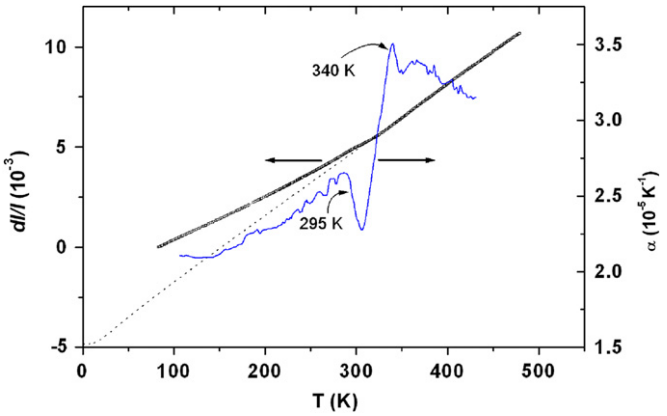

Fig. 4. Temperature dependence of the linear thermal expansion and thermal expansion coefficient α versus temperature for $ErMn_6Sn_6$ sample. The dashed line shows the simulated phonon contribution (Grüneisen law) using $\theta_D=102$ K.

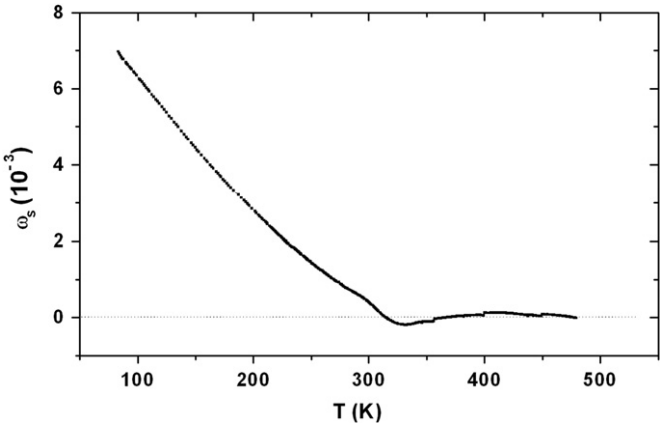

Fig. 5. Temperature dependence of the spontaneous volume magnetostriction ω_s.

about 200 μm and minor impurity phases in grain boundaries, consistent with the XRD results.

The ac magnetic susceptibility χ_{ac} of the studied sample in a zero dc magnetic field in the temperature range of 77–330 K is presented in Fig. 3. This thermomagnetic curve (which is frequency independent) is characterized by a strong increase of magnetization at low temperature, without displaying the exact ordering point. However, transition temperatures have been taken from the anomalies in its first derivative curve. This behavior was expected and can be explained as follows: at low temperature, the Er–Mn strong antiferromagnetic coupling, which as said, is very sensitive to the Mn–Mn interatomic distances, dominates the Mn–Mn one and so causes the Er and Mn sublattices to order ferromagnetically in the (001) plane, resulting in a collinear ferrimagnetic order [4]. Hence, the 77 K ordering point may be attributed to the ordering of the Er sublattice. As temperature increases, the Er–Mn interaction weakens due to thermal expansion, so Mn–Mn coupling dominates. Therefore, the Mn sublattice orders antiferromagnetically and the Er sublattice is in the paramagnetic state, resulting in an antiferromagnetic order between 77 K and about 330 K (330 K was the highest available temperature in this measurement around which TE reveals a notable steep change, indicating a probable transition at a temperature a little higher than 330 K). It may be also seen from Fig. 3 that a distinct feature appears at about 160 K. The first possible origin of this anomaly may be the presence of some magnetic impurity phase in the sample. However, this is less likely, because a phase with such a pronounced peak would have been detected easily in the XRD pattern of the sample (the magnetic transition temperatures of the detected minor phases do not correspond to this point: β-Sn is paramagnetic, Er_2O_3 has a transition at $T_N=3.4$ K and Mn_3Sn_2 at $T_{C1}=262$ and $T_{C2}=227$ K). This not being the case, we can conclude that it is a feature belonging to the main phase needing further investigation.

Fig. 4 shows the temperature dependence of the zero-field linear thermal expansion dl/l of the studied sample in the range of 77–480 K. It displays a metallic behavior with a change of slope at about 332 K (see the temperature dependence of the thermal expansion coefficient α of the sample, depicted by taking a point-to-point temperature derivative of the dl/l data). However, anomalous behavior of α extends over the temperature interval of 295–340 K, namely from the onset of the antiferromagnetic-paramagnetic transition to the point where this phenomenon is completed. The magnetic contribution to the thermal expansion $(dl/l)_m$ can be estimated from the difference between the observed dl/l curve and the usual anharmonic phonon contribution governed by the Grüneisen law using $\theta_D=102$ K derived from the specific heat data [15]. The calculated nonmagnetic contribution that has been fitted to the experimental results in the paramagnetic regime is depicted in Fig. 4 as a dashed line. Assuming that the linear thermal expansion dl/l is isotropic, the spontaneous volume magnetostriction is $\omega_s=3(dl/l)_m$. The temperature dependence of the ω_s values is shown in Fig. 5. The observed significant volume expansion at about 340 K, where the ac susceptibility is going to reveal an anomaly, too, should be due to transition of the Mn sublattice to the antiferromagnetic order. It is believed and also confirmed by the present χ_{ac} measurements that at about 77 K, the Er sublattice moments in $ErMn_6Sn_6$ align ferromagnetically, but as seen this alignment does not cause any notable anomaly in the thermal expansion behavior. These observations and the above discussion indicate a $T_N=340$ K and $T_C\approx 77$ K for this $ErMn_6Sn_6$ sample, close to the 352 and 75 K values suggested by Venturini et al. [1]. The insignificant spontaneous magnetostriction effects in the paramagnetic phase should be due to the existence of short-range magnetic correlations above the ordering temperature.

The longitudinal $\lambda_{\parallel}$ and transverse magnetostriction $\lambda_{\perp}$ of the sample were measured as a function of the applied field for some typical temperatures. Except for the region about the antiferromagnetic–ferrimagnetic transition point, there is no significant difference between the MS measured parallel and perpendicular to the applied magnetic field (as representative, the $\lambda_{\parallel}$, $\lambda_{\perp}$ and anisotropic magnetostriction $\lambda_t=\lambda_{\parallel}-\lambda_{\perp}$ isotherms at two selected temperatures are presented in Fig. 6). This indicates that the magnetostriction is almost isotropic and as suggested for the similar behavior observed in $GdMn_2Ge_2$ [16],

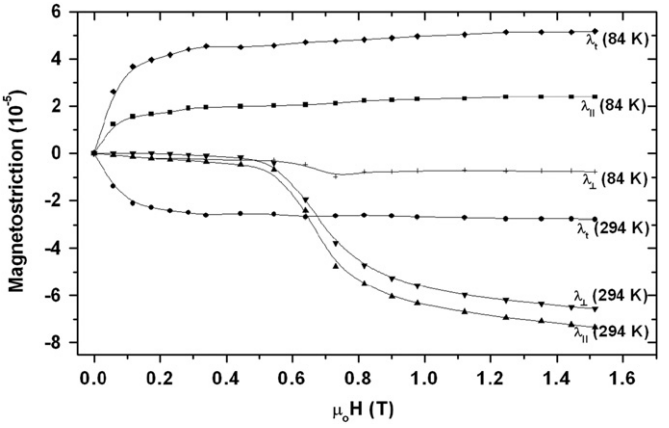

Fig. 6. Longitudinal $\lambda_{||}$, transverse $\lambda_\perp$ and anisotropic magnetostriction $\lambda_t=\lambda_{||}-\lambda_\perp$ isotherms of the sample as a function of applied magnetic field at the selected temperatures of 84 K and room temperature. In this and the following figures, the lines connecting the data points are only guides for the eye.

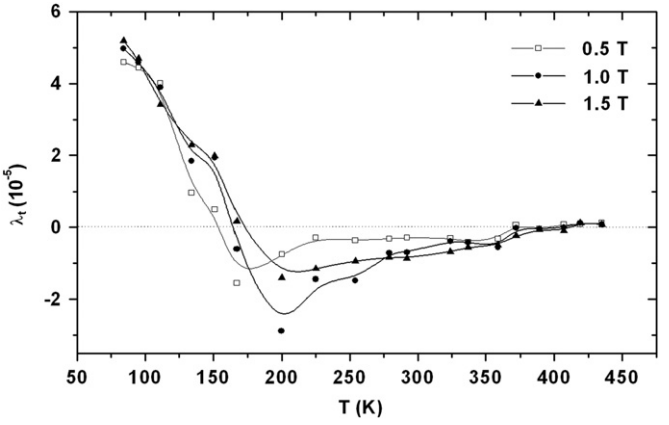

Fig. 7. Temperature dependence of the anisotropic magnetostriction of the $ErMn_6Sn_6$ sample at the selected magnetic fields of 0.5, 1.0 and 1.5 T.

mainly caused by interlayer Mn–Mn exchange interaction. The small difference between $\lambda_{||}$ and $\lambda_\perp$ may come from the textural structure of polycrystalline sample. Fig. 7 shows the temperature dependence of the anisotropic magnetostriction λ_t at some typical applied magnetic field. As seen, λ_t is almost field-independent and from $\lambda_t \sim O(10^{-4})$ at low temperatures it drops continuously to zero at about $T_p=160$ K due to magnetostriction compensation of the two sublattices involved in the MS effect. Above this point, λ_t shows a sign change and then tends to zero once again around 360 K (close to T_N of the sample). From the negative values of λ_t above the compensation point (T_p) where Er sublattice is in its paramagnetic state and MS originates from the Mn sublattice anisotropy, one can conclude that the Er and Mn sublattices contributions to the MS of this sample are positive and negative, respectively.

For further discussion, we consider the magnetostriction relation for a hexagonal structure in terms of magnetostrictive coefficients $\lambda_i^{\mu,l}$ describing the strain measurement in a direction with cosines of β_i ($i=x$, y and z) when magnetization is in a direction described by cosines α_i ($i=x$, y and z) [17]:

$$\lambda=\lambda_1^{\alpha,0}(\beta_x^2+\beta_y^2)+\lambda_2^{\alpha,0}\beta_z^2+\lambda_1^{\alpha,2}(\beta_x^2+\beta_y^2)(\alpha_z^2-\tfrac{1}{3})+\lambda_2^{\alpha,2}\beta_z^2(\alpha_z^2-\tfrac{1}{3})$$
$$+\lambda^{\gamma,2}\left\{\frac{1}{2}(\beta_x^2-\beta_y^2)(\alpha_x^2-\alpha_y^2)+2\beta_x\beta_y\alpha_x\alpha_y\right\}+2\lambda^{\varepsilon,2}(\beta_x\alpha_x+\beta_y\alpha_y)\beta_z\alpha_z \quad (1)$$

Here in $\lambda_i^{\mu,l}$, the first superscript $\mu=\alpha$ indicates the fully symmetric volume change (with preservation of hexagonal symmetry), and $\mu=\gamma$ and ε represent shearing strains in the basal plane and in planes parallel to the c-axis, respectively. The second superscript l denotes the degree of magnetization direction cosines pertaining to that particular term, i.e. $\lambda_i^{\mu,0}$ coefficients are terms independent of magnetization direction and $\lambda_i^{\mu,2}$ ones are quadratic in magnetization direction cosines. In a single crystal sample, all λ_i coefficients are responsible for the different types of deformation and distortion, while for a polycrystalline sample, the MS expression must be averaged over all directions within a sphere. Following Mason [18], we derive the anisotropic magnetostriction expression for a polycrystalline hexagonal sample as:

$$\lambda_t=\lambda_{||}-\lambda_\perp=\frac{2}{15}(-\lambda_1^{\alpha,2}+\lambda_2^{\alpha,2})+\frac{2}{5}(\lambda^{\gamma,2}+2\lambda^{\varepsilon,2}) \quad (2)$$

where $\lambda_1^{\alpha,2}$ (and $\lambda_2^{\alpha,2}$) refers to the distortion in the basal plane (and along the c-axis) upon the magnetization rotation from the basal plane to the c-axis (and from the c-axis to the basal plane). These two modes maintaining the hexagonal symmetry are associated with a volume change and a change in the c/a ratio for fixed volume. The $\lambda^{\gamma,2}$ and $\lambda^{\varepsilon,2}$ denote a breaking of the circular symmetry of the basal plane by magnetization rotation in the plane and a distortion in the angle 90° between the c-axis and the basal plane, respectively. For the present sample, which is an easy plane compound with high anisotropy field, the magnetization rotation in low temperatures and fields is restricted to the basal plane. Therefore, on account of the above discussion, $\lambda^{\gamma,2}$ is the dominant term in the conditions of low temperatures and fields. Hence, from the outline presented here, one can conclude that $\lambda^{\gamma,2}$ is positive for this compound. As the temperature increases and consequently the planar anisotropy field decreases, the magnetization vector senses all directions. So, using the Eq. (2) and considering that $\lambda^{\varepsilon,2}$ can be neglected in easy plane compounds, like the sample in the present study, we conclude that at higher temperatures $(-\lambda_1^{\alpha,2}+\lambda_2^{\alpha,2})$ is negative for $ErMn_6Sn_6$.

The temperature dependence of the volume magnetostriction ω at selected applied magnetic fields is represented in Fig. 8. As seen, in contrast to λ_t behavior, ω depends strongly on the magnitude of the applied field in the temperature range of 77–340 K, i.e. in the antiferromagnetic state where the Mn sublattice has an antiferromagnetic ordering and the Er one is in a paramagnetic state. The antiferromagnetic state of $ErMn_6Sn_6$ at low temperatures, i.e. close to the ordering point of Er sublattice, is not very stable and may be transformed easily by application of a magnetic field strong enough to overcome the

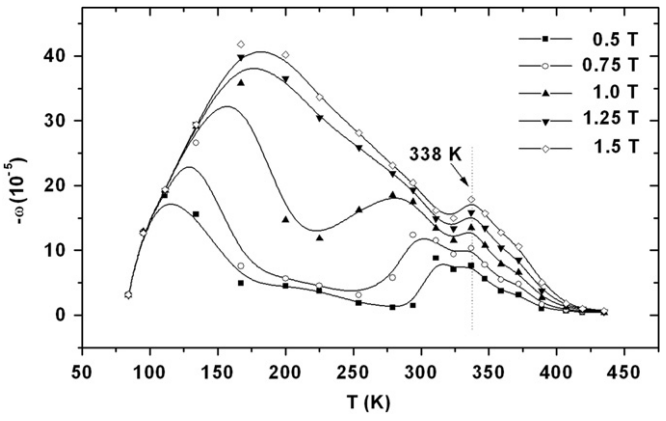

Fig. 8. Temperature dependence of the volume magnetostriction ω of the $ErMn_6Sn_6$ sample at the selected magnetic fields of 0.5, 0.75, 1.0, 1.25 and 1.5 T.

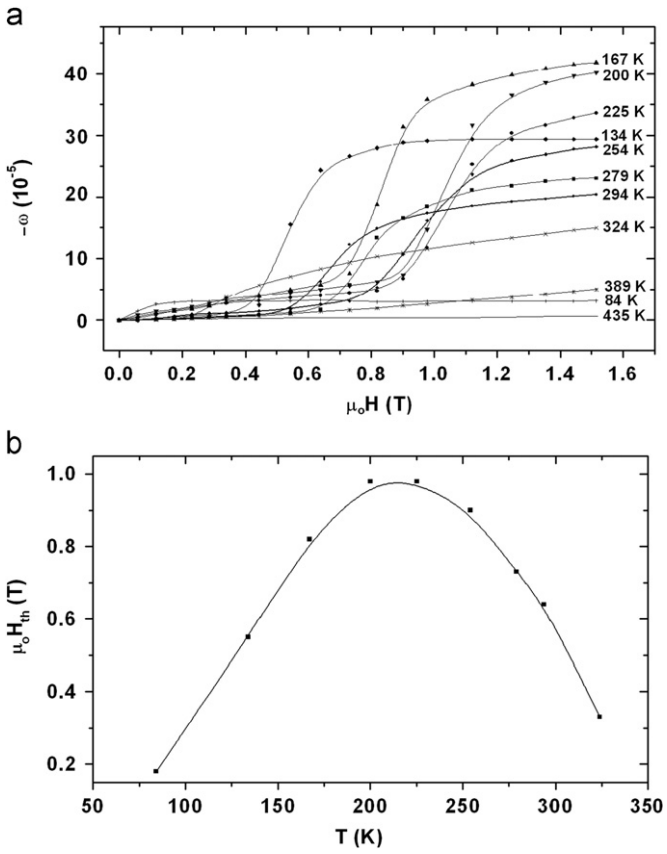

Fig. 9. (a) Volume magnetostriction isotherms of $ErMn_6Sn_6$ sample versus applied magnetic field at some selected temperatures. (b) Thermal variation of the threshold magnetic field for antiferromagnetic–ferrimagnetic transition H_{th} derived from derivative of the ω isotherms curves.

sublattice molecular field and force the Mn sublattice moments to flip to the ferromagnetic state. Due to the strong antiferromagnetic Er–Mn coupling, this in turn forces the Er ones to order ferromagnetically and antiferromagnetically to the Mn ones, resulting in a transition to the ferrimagnetic state, which is accompanied by a notable decrease in the unit-cell volume. It is readily seen that at lower temperatures, ω shows a rapid increase with temperature, and its maximum value moves to higher temperatures by increasing the applied magnetic field. Then with further temperature increase, ω decreases until about T_N, where it logically peaks. As temperature increases, the threshold magnetic field for the antiferromagnetic–ferrimagnetic transition H_{th} increases. The thermal variation of the H_{th} derived from the maximum slope of the ω isotherms (Fig. 9a), or in other words, where the magnetostriction susceptibility peaks, is presented in Fig. 9b. As seen, it increases from 0.18 T at 84 K to about 1.0 T at 225 K and then decreases to T_N. The thermal variation of H_{th} is well consistent with the result deduced from the maximum slope of the magnetization isotherms reported by Hu et al. [14], where this behavior has been attributed to an exchange-related metamagnetic transition, rather than the anisotropy-related one. Furthermore, the low H_{th} values indicate that the Mn–Mn coupling in $ErMn_6Sn_6$ compound is not very strong, compared with most of RMn_6Ge_6 [19] and some of other RMn_6Sn_6 compounds like R=Tm and nonmagnetic R's [2]. As seen in Fig. 8, similar to the α anomalous behavior (Fig. 4), the ω anomalous behavior due to this metamagnetic antiferromagnetic–ferrimagnetic transition extends over a temperature interval, i.e. from the onset of this transition to the point where it is completed. However, as seen, with increasing applied magnetic field, the temperature range of the antiferromagnetic state narrows: with increasing applied magnetic field, the low temperature transition shifts to higher temperatures, while the high temperature one occurs at lower temperatures. Meanwhile, the transition to the paramagnetic state undergoes no change (at T_N=338 K). This is well expected from the magnetic phase diagram of $ErMn_6Sn_6$ [2].

For further discussion on volume magnetostriction of this compound (Fig. 8), note that in Relation (1), the first two terms ($\lambda_1^{\alpha,0}$ and $\lambda_2^{\alpha,0}$) arising from the two-ion isotropic exchange interactions, depend only on the magnitude of magnetization (or the applied magnetic field), and not on its direction. So, the volume change of the sample independent of the magnetization direction is governed by $(2\lambda_1^{\alpha,0}+\lambda_2^{\alpha,0})$, while other terms describe modes of anisotropic MS; $(2\lambda_1^{\alpha,2}+\lambda_2^{\alpha,2})$ $(\alpha_z^2|_{final}-\alpha_z^2|_{initial})$ is related to the volume change due to the magnetization rotation [17]. At low temperatures and applied fields, as the magnetic moments of the sample are restricted to the basal plane, there is no magnetization direction-dependent contribution to the volume change. Therefore, at the condition of low temperatures and fields, the ω of $ErMn_6Sn_6$ sample depends only on the variation of magnetization magnitude with temperature and applied magnetic field changes. Hence, one can conclude from the observed ω behavior that the quantity $(2\lambda_1^{\alpha,0}+\lambda_2^{\alpha,0})$ is negative for this compound. Furthermore, previous reports on the magnetization of this compound [6] show that it has its highest values around 100, 120 and 150 K under applied magnetic fields of 0.5, 1.0 and 1.5 T, respectively. Hence, consistent with the above discussion, the observed maxima in the thermal behavior of ω (Fig. 8) correspond to the variations of magnetization with temperature and applied magnetic field. The magnetization decreasing after these points due to the increase in the threshold field for metamagnetic transition from antiferromagnetic to ferrimagnetic state (H_{th}) brings about a decrease in ω. The H_{th} decrease at higher temperature causes an increase in the magnetization and consequently in ω around T_N.

4. Conclusions

The almost pure single-phase polycrystalline sample of $ErMn_6Sn_6$ intermetallic compound was prepared by the arc melting method. The compound possesses a hexagonal $HfFe_6Ge_6$-type structure (S.G. P6/mmm) with the refined lattice parameters a=5.527(4) and c=9.020(4) Å. The magnetostriction and thermal expansion of sample have been investigated in the temperature range of 77 K to above 400 K. The thermal expansion measurement of the sample shows anomalous behavior around its T_N=340 K. The isofield curves of volume magnetostriction peak at paramagnetic–antiferromagnetic and antiferromagnetic–ferrimagnetic phase transitions. In the antiferromagnetic state, the transition to ferrimagnetism can be induced by an applied magnetic field. This threshold field for the metamagnetic transition H_{th} increases from 0.18 T at 84 K to about 1 T around 220 K, and then decreases monotonously to T_N. This behavior is well consistent with that observed earlier on magnetization curves being attributed to the exchange-related metamagnetic transition rather than the anisotropy-related one. Furthermore, the low H_{th} values suggest that the Mn–Mn coupling in $ErMn_6Sn_6$ is not so strong. The experimental results obtained were discussed in the framework of two-magnetic sublattice by accounting for the lattice parameter dependence of the interlayer Mn–Mn exchange interaction in this layered compound. From the temperature dependence of magnetostriction measurements and considering the magnetostriction relation of a hexagonal structure, the signs of some of the magnetostriction constants were determined.

References

[1] G. Venturini, B. Chafik El Idrissi, B. Malaman, Journal of Magnetism and Magnetic Materials 94 (1991) 35.
[2] D.M. Clatterbuck, K.A. Gschneidner Jr., Journal of Magnetism and Magnetic Materials 207 (1999) 78.
[3] K. Suga, K. Kindo, L. Zhang, E. Brück, K.H.J. Buschow, F.R. de Boer, C. Lefèvre, G. Venturini, Journal of Alloys and Compounds 408–412 (2006) 158.
[4] B. Malaman, G. Venturini, R. Welter, J.P. Sanchez, P. Vulliet, E. Ressouche, Journal of Magnetism and Magnetic Materials 202 (1999) 519.
[5] K. Shimizu, T. Hori, Journal of Magnetism and Magnetic Materials 310 (2007) 1874.
[6] Jin-lei Yao, Shao-ying Zhang, Bao-dan Liu, Bao-gen Shen, Ru-wu Wang Li-gang Zhang, De-ren Yang, Mi Yan, Journal of Applied Physics 95 (2004) 7061.
[7] D.M. Clatterbuck, R.J. Lange, K.A. Gschneidner Jr., Journal of Magnetism and Magnetic Materials 195 (1999) 639.
[8] T. Mazet, J. Tobola, G. Venturini, B. Malaman, Physical Review B 65 (104406) (2002) 1.
[9] F. Canepa, R. Duraj, C. Lefèvre, B. Malaman, A. Mar, T. Mazet, M. Napoletano, A. Szytula, J. Tobola, G. Venturini, A. Vernière, Journal of Alloys and Compounds 383 (2004) 10.
[10] J.H.V.J. Brabers, A.J. Nolten, F. Kayzel, S.H.J. Lenczowski, K.H.J. Buschow, F.R. de Boer, Physical Review B 50 (22) (1994) 16410.
[11] Jin-lei Yao, Shao-ying Zang, Lu Li, Tao Zhu, Mi yan, De-ren Yang, Bao-gen Shen, Journal of Applied Physics 93 (2003) 6984.
[12] G. Venturini, Journal of Alloys and Compounds 400 (2005) 37.
[13] T. Roisnel, J. Rodríguez-Carvajal, Materials Science Forum 378–381 (2001) 118.
[14] Jifan Hu, Fuming Yang, Yizhong Wang, Jianli Wang, F.R. de Boer, Physica Status Solidi (b) 214 (1999) 135.
[15] H.G.M. Duijn, Ph.D. Thesis, Universiteit van Amsterdam, 2000, p. 141.
[16] Guo Guang-Hua, Wu Ye, Zhang Hai-Bei, D.A. Filippov, R.Z. Levitin, V.V. Snegirev, Chinese Physics 11 (2002) 608.
[17] A.E. Clark, B.F. DeSavage, R. Bozorth, Physial Review 138 (1965) A216.
[18] W.P. Mason, Physical Review 96 (1954) 302.
[19] G. Venturini, R. Welter, B. Malaman, Journal of Alloys and Compounds 185 (1992) 99.